

1    Faecal virome transplantation decrease symptoms of type-2-  
2    diabetes and obesity in a murine model

3    Torben Sølbeck Rasmussen<sup>1\*</sup>, Caroline M. Junker Mentzel<sup>2</sup>, Witold Kot<sup>3</sup>, Josué L. Castro-  
4    Mejía<sup>1</sup>, Simone Zuffa<sup>4</sup>, Jonathan Swann<sup>4</sup>, Lars Hestbjerg Hansen<sup>3</sup>, Finn Kvist Vogensen<sup>1</sup>,  
5    Axel Kornerup Hansen<sup>2\*</sup>, Dennis Sandris Nielsen<sup>1\*</sup>

6    **Author affiliations**

7    <sup>1</sup> Section of Microbiology and Fermentation, Dept. of Food Science, University of Copenhagen, Frederiksberg, Denmark

8    <sup>2</sup> Section of Experimental Animal Models, Dept. of Veterinary and Animal Sciences, University of Copenhagen,  
9    Frederiksberg, Denmark

10    <sup>3</sup> Section of Microbial Ecology and Biotechnology, Department of Plant and Environmental Sciences, University of  
11    Copenhagen, Frederiksberg, Denmark

12    <sup>4</sup> Department of Metabolism, Digestion and Reproduction, Faculty of Medicine, Imperial College, London, United  
13    Kingdom

14    \*Address correspondence to [dn@food.ku.dk](mailto:dn@food.ku.dk) (+45 35 33 32 87) / [torben@food.ku.dk](mailto:torben@food.ku.dk) (+45 35 32 80 73), Rolighedsvej 26  
15    4th floor, 1958 Frederiksberg C, Denmark.

16

17 **ABSTRACT**

18 **Objective:** Development of obesity and type-2-diabetes (T2D) are associated with gut microbiota  
19 (GM) changes. The gut viral community is predominated by bacteriophages (phages), which are  
20 viruses that attack bacteria in a host-specific manner. As a proof-of-concept we demonstrate the  
21 efficacy of faecal virome transplantation (FVT) from lean donors for shifting the phenotype of obese  
22 mice into closer resemblance of lean mice.

23 **Design:** The FVT consisted of viromes extracted from the caecal content of mice fed a low-fat (LF)  
24 diet for fourteen weeks. Male C57BL/6NTac mice were divided into five groups: LF (as control),  
25 high-fat diet (HF), HF+Ampicillin (Amp), HF+Amp+FVT and HF+FVT. At week six and seven of the  
26 study the HF+FVT and HF+Amp+FVT mice were treated with FVT by oral gavage. The Amp  
27 groups were treated with ampicillin 24 h prior to first FVT treatment.

28 **Results:** Six weeks after first FVT the HF+FVT mice showed a significant decrease in weight gain  
29 compared to the HF group. Further, glucose tolerance was comparable between the lean LF and  
30 HF+FVT mice, while the other HF groups all had impaired glucose tolerance. These observations  
31 were supported by significant shifts in GM composition, blood plasma metabolome, and expression  
32 levels of genes involved in obesity and T2D development.

33 **Conclusions:** Transfer of gut viral communities from mice with a lean phenotype into those with an  
34 obese phenotype reduce weight gain and normalise blood glucose parameters relative to lean  
35 mice. We hypothesise that this effect is mediated via FVT-induced GM changes.

36

37 **Key words:** Obesity; type-2-diabetes; gut virome; bacteriophages; gut microbiota; metabolomics

38

39 **Significance of this study**

40 What is already known about this subject?

- 41 • Obesity and type-2-diabetes (T2D) are associated with gut microbiota (GM) dysbiosis.
- 42 • Faecal microbiota transplant from lean donors has previously shown potential in treating
- 43 obesity and T2D.
- 44 • Patients suffering from recurrent *Clostridium difficile* infections (rCDI) have been cured with
- 45 sterile filtered donor faeces (containing enteric viruses and no bacteria), here defined as
- 46 faecal virome transplantation (FVT).

47 What are the new findings?

- 48 • FVT from lean donors lead to decreased weight gain and normalised blood sugar tolerance
- 49 in a diet-induced obesity (DIO) mouse model.
- 50 • FVT significantly changed the bacterial and viral GM component, as well as the plasma
- 51 metabolome and the expression profiles of obesity and T2D associated genes.
- 52 • Initial treatment with ampicillin prior FVT seems to counteract the beneficial effects
- 53 associated with FVT.

54 How might it impact on clinical practice in the foreseeable future?

- 55 • We here show a proof-of-concept, providing a solid base for designing a clinical study of
- 56 FVT targeting obesity and T2D in humans. This is further augmented by the increased
- 57 safety related to FVT, since bacteria and other microorganisms are removed from the donor
- 58 faeces, and therefore minimises the risk of disease transmission.
- 59 • These findings highlight the potential application of FVT treatment of various diseases
- 60 related to GM dysbiosis and further support the vital role of the viral community in
- 61 maintaining and shaping the GM.

62

63 **INTRODUCTION**

64 Obesity and type-2-diabetes (T2D) constitute a world-wide health threat[1]. During the last decade  
65 it has become evident that certain diseases, including obesity and T2D, are associated with gut  
66 microbiota (GM) dysbiosis[2]. Interestingly, germ free (GF) mice do not develop diet-induced-  
67 obesity (DIO)[3], but when exposed to faecal microbiota transplantation (FMT) from an obese  
68 human donor they increase their body weight significantly more compared to GF mice exposed to  
69 FMT from a lean donor[4]. At present FMT is widely used to efficiently treat recurrent *Clostridium*  
70 *difficile* infections (rCDI)[5], and is suggested to have therapeutic potential against metabolic  
71 syndrome, a condition related to obesity and T2D[6]. FMT is considered as a safe treatment,  
72 however, safety issues remain since screening methods cannot fully prevent adverse effects  
73 caused by disease transmission from the donor faeces[7]. A failure in the screening procedure  
74 caused recently in a death (June 2019) of a patient following FMT[8] due to a bacterial infection.

75 The gut viral community (virome) is dominated by prokaryotic viruses[9], also called  
76 bacteriophages (phages), which are viruses that attack bacteria in a host-specific manner[10].  
77 During recent years, evidence has mounted that the gut virome plays a key role in shaping the  
78 composition of the GM[11,12] as well as influencing the host metabolome[13]. Interestingly, rCDI  
79 have been successfully treated with a transfer of filtered donor faeces (containing phages, but no  
80 intact bacterial cells)[14]. Five out of five patients were successfully treated[14]. This approach is  
81 referred to as faecal virome transplantation (FVT). Further, antibiotic treatment alters the GM  
82 composition, but Draper *et al.* 2019 recently showed that the murine GM can be reshaped with  
83 FVT after antibiotic treatment[15].

84 DIO mice is a common animal model of metabolic syndrome, including symptoms such as obesity  
85 and insulin resistance/pre-T2D[16]. With C57BL/6NTac mice as the model, we hypothesised that  
86 FVT (originating from lean healthy donor mice) treatment of DIO mice would change the GM  
87 composition and directly or indirectly counteract the symptoms of obesity and T2D. To the best of  
88 our knowledge, this is the first study investigating the effect of FVT targeting obesity and T2D.

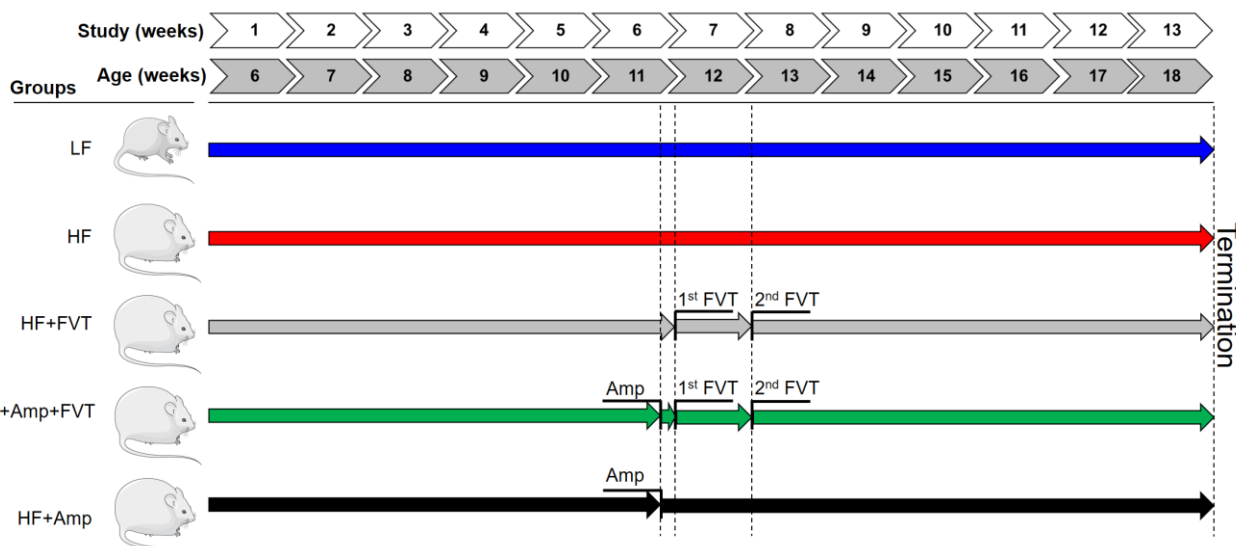
89

90 **METHODS**

91 Detailed methods are enclosed in the online supplementary materials.

92 **Animal study design**

93 Forty male C57BL/6NTac mice (Taconic Biosciences A/S, Lille Skensved, Denmark) were divided  
94 into 5 groups at 5 weeks of age: low-fat diet (LF, as lean control), high-fat diet (HF), HF+Ampicillin  
95 (Amp), HF+Amp+FVT and HF+FVT (Figure 1). For thirteen weeks  
96 mice were fed *ad libitum* a HF diet (Research Diets D12492, USA) or a LF diet (Research Diets  
97 D12450J, USA). After six weeks on their respective diets, the HF+FVT and HF+Amp+FVT mice  
98 were treated twice with 0.15 mL FVT by oral gavage with a one-week interval (week 6 and 7)  
99 between the FVT. On the day before the first FVT inoculation the HF+Amp and HF+Amp+FVT  
100 animals were treated with a single dose of ampicillin (1 g/L) in the drinking water. The FVT viromes  
101 were extracted from the caecal content of eighteen mice fed a LF diet for 14 weeks, that were  
102 earlier isolated, sequenced, and analysed[17].



103

104 *Figure 1: Experimental setup of the faecal virome transplantation (FVT). Forty male C57BL/6NTac mice (5 weeks old)*  
105 *were divided into five groups: Low-fat diet (LF, as healthy control), High-fat diet (HF), HF+Ampicillin (Amp),*  
106 *HF+Amp+FVT and HF+FVT. Their respective diets were provided continuously for 13 weeks until termination (18 weeks*  
107 *old). The HF+FVT and HF+Amp+FVT mice were treated with FVT twice with one-week interval by oral gavage at week 6*  
108 *and 7 of the study. Ampicillin was added once to the drinking water one day before first FVT (week 6) for HF+Amp and*  
109 *HF+Amp+FVT. Mouse icon originates from <https://smart.servier.com/> under the CC BY 3.0 license.*

110 The titer of the FVT viromes was approximately  $2 \times 10^{10}$  Virus-Like-Particles/mL (FigureS1). The  
111 mice were subjected to an oral glucose tolerance test (OGTT)[18] at week 12 of the study and food  
112 intake and mouse weight was monitored. The study was approved by the Danish Competent  
113 Authority, The Animal Experimentation Inspectorate, under the Ministry of Environment and Food  
114 of Denmark, and performed under license No. 2017-15-0201-01262 C1-3. Procedures were carried

115 out in accordance with the Directive 2010/63/EU and the Danish law LBK Nr 726 af 09/091993,  
116 and housing conditions as earlier described[17]. Blood plasma, intestinal content from the cecum  
117 and colon as well as tissue from the liver and ileum were sampled at termination at week 13 (18  
118 weeks old). Mouse data (weight, OGTT levels, etc.) were analysed in GraphPad Prism using one-  
119 way ANOVA with Tukeys test.

## 120 **Pre-processing of faecal samples**

121 This study included in total 79 intestinal content samples, of which 40 were isolated from cecum  
122 and 39 from colon. Pre-processing was performed as earlier described[17].

## 123 **Bacterial DNA extraction, sequencing, and pre-processing of raw data**

124 Tag-encoded 16S rRNA gene amplicon sequencing was performed on an Illumina NextSeq using  
125 v2 MID output 2x150 cycles chemistry (Illumina, CA, USA). DNA extraction and library building for  
126 amplicon sequencing was performed in accordance with Krych *et al.*[19]. The average sequencing  
127 depth (Accession: PRJEB32560, available at ENA) for the cecum 16S rRNA gene amplicons was  
128 164,147 reads (min. 22,732 reads and max. 200,2003 reads) and 166,012 reads for colon (min.  
129 89,528 reads and max. 207,924 reads) (TableS1). bOTU tables (bacterial-operational taxonomic  
130 units) were generated and taxonomy assigned as earlier described[17]. Bacterial density of the  
131 caecal and colon content was estimated by quantitative real-time polymerase chain reaction  
132 (qPCR) as previously described[20], using the 16S rRNA gene primers (V3 region) also applied for  
133 the amplicon sequencing[19].

## 134 **Viral DNA extraction, sequencing and pre-processing of raw data**

135 The enteric viral community was purified, DNA extracted and the gut metavirome determined as  
136 previously described[17]. The average sequencing depth (Accession: PRJEB32560, available at  
137 ENA) for the cecum viral metagenome was 612,640 reads/sample (min. 277,582 reads and max.  
138 1,219,178 reads) and 356,976 reads/sample for colon (min. 33,773 reads and max. 584,681 reads)  
139 (TableS1). For each sample, reads were treated with Trimmomatic[21] and Usearch[22] and  
140 subjected to within-sample *de novo* assembly with MetaSpades v.3.5.0[23,24]. Viral contigs were  
141 identified with Kraken2[25], VirFinder[26], PHASTER[27], and virus orthologous proteins  
142 ([www.vogdb.org](http://www.vogdb.org)). Contaminations of non-viral contigs like bacteria, human, mice, and plant DNA  
143 were removed (FigureS2). The remaining contigs constituted the vOTU (viral-operational  
144 taxonomic unit) table.

## 145 **Gene expression assay**

146 Genes investigated for expression analysis were selected based on relevant pathways for each  
147 tissue. For the liver, genes involved in metabolic pathways (triglyceride, carbohydrate, bile and

148 cholesterol metabolism) and inflammation were selected. For the ileum, genes involved in  
149 inflammation, gut microbiota signalling and gut barrier function were selected [28,29]. Primer  
150 sequences are listed in Table S2. qPCR was performed using the Biomark HD system (Fluidigm  
151 Corporation) on 2x 96.96 IFC chips on pre-amplified cDNA duplicates following the instructions of  
152 the manufacturer with minor adjustments as previously described[30]. Gene expression data was  
153 analysed in R using linear models (one-way ANOVA) with either HF or LF as control groups.

#### 154 **Blood plasma metabolome analysis**

155 Plasma samples were prepared for ultra-performance liquid chromatography mass spectrometry  
156 (UPLC-MS) analysis according to a previously published protocol[31]. Principal component  
157 analysis (PCA) and orthogonal projection to latent structures-discriminant analysis (OPLS-DA)  
158 models were built on the plasma metabolic profiles to identify biochemical variation between the  
159 groups. Among the features driving the different OPLS-DA models, only those with variable  
160 importance in the projection (VIP) scores  $> 2$  were further investigated. Putative annotation was  
161 achieved through searching for the m/z values in online databases such as HMDB  
162 (<http://www.hmdb.ca>), METLIN (<http://metlin.scripps.edu>) and Lipidmaps  
163 (<http://www.lipidmaps.org>). Additionally, fragmentation patterns derived from MS<sup>e</sup> experiment were  
164 compared to online spectra when available.

#### 165 **Bioinformatic analysis of bacterial and viral DNA**

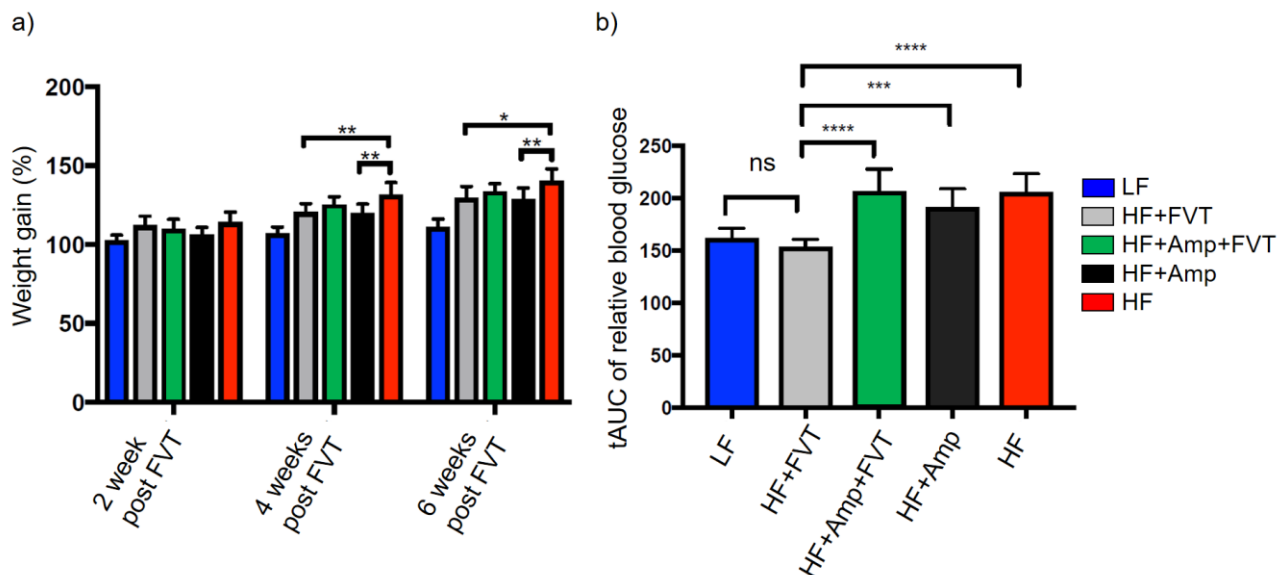
166 Prior to any analysis the raw read counts in vOTU-tables were normalised by reads per kilo base  
167 per million mapped reads (RPKM)[32]. b- and vOTU's that were detected in less than 8% of the  
168 samples were discarded to reduce noise while still maintaining an average total abundance close  
169 to 98%. ANOSIM and Kruskal Wallis was used to evaluate multiple group comparisons.  
170 Regularised Canonical Correlation Analysis (rCCA) was performed with mixOmics v. 6.8.0. R-  
171 package[33] to predict correlations between bacterial and viral taxa. Only vOTUs  $\geq 5000$  bp were  
172 included in the rCCA. The machine learning algorithm random forest[34] was applied to select  
173 variables explaining the dataset and normalised in range of -1:1 ((x-mean)/max(abs(x-mean))) and  
174 visualised by Heatmap3[35].

## 175 **RESULTS**

176 Here we investigated the potential of faecal virome transplantation (FVT) to shift the phenotype of  
177 obesity and T2D in DIO male C57BL/6NTac mice towards a lean mice phenotype. Intestinal  
178 contents from the cecum and colon were isolated, but here only results from the cecum samples  
179 are be reported. Complete equivalent analysis of colon samples can be found in Figure S10.

180 **FVT from lean donor decreases weight gain and normalises blood glucose tolerance  
181 in DIO mice**

182 Mice were weighed pre and post FVT with 1-2 weeks of interval. At both 4- and 6-weeks post first  
183 FVT (15 and 17 weeks old) a significantly lower body weight gain was observed in the HF+FVT ( $p$   
184  $< 0.017$ ) and the HF+Amp mice ( $p < 0.006$ ) compared to the HF mice (Figure 2a). Intriguingly,  
185 OGTT showed no significant differences ( $p > 0.842$ ) between the LF and the HF+FVT mice, while  
186 the OGTT level of the HF mice was significantly increased ( $p < 0.0001$ ) compared to both the LF  
187 and HF+FVT group suggesting that FVT had normalised the blood glucose tolerance in the  
188 HF+FVT mice (Figure 2b). Furthermore, the OGTT of HF+Amp+FVT was comparable to the HF  
189 mice ( $p > 0.999$ ), indicating that the initial disruption of the bacterial composition by the ampicillin  
190 treatment had counteracted the effect of the FVT in the HF+Amp+FVT mice. Which simultaneously  
191 suggest that the effects associated to the FVT occurs via alterations in the GM component. Non-  
192 fasted blood glucose was measured regularly in addition to HbA1c levels and food consumption pr.  
193 cage (FigureS4).



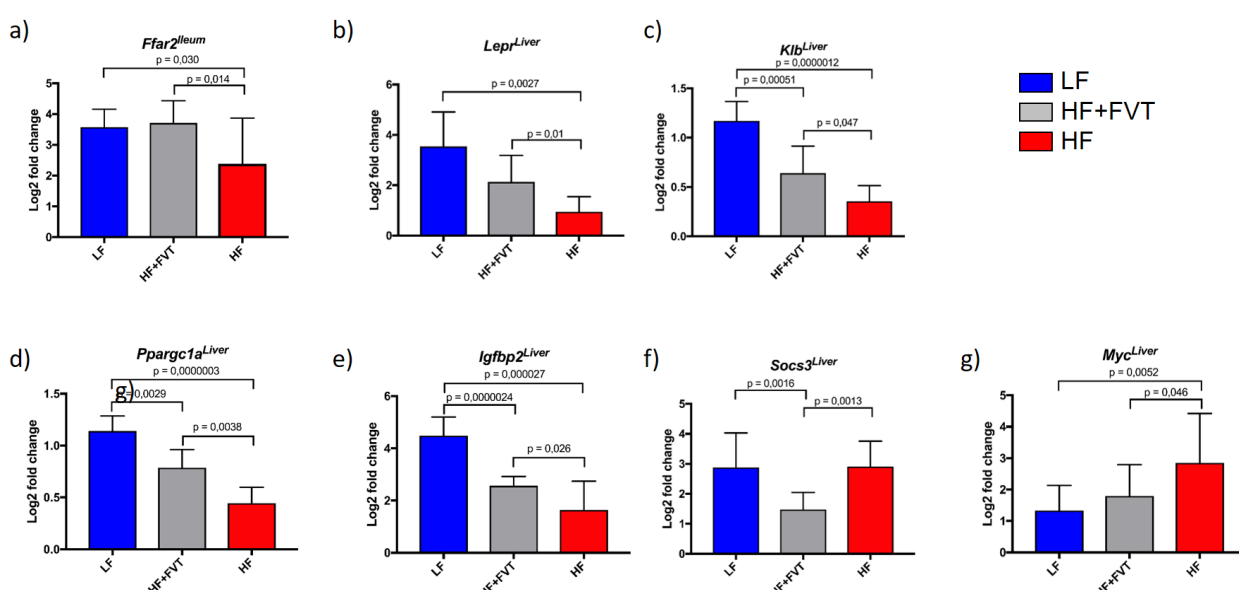
194

195 *Figure 2: a) Bar plot of body weight gain measured at 2, 4, and 6 weeks (13, 15, 17 weeks old respectively) post first  
196 faecal virome transplantation (FVT). b) Oral glucose tolerance test (OGTT) levels measured 6 weeks post first FVT (17  
197 weeks old). Values are based on the total area under curve (tAUC) relatively to the blood glucose levels of the individual  
198 mouse. Significant differences of the pairwise comparison at week 4 and 6 post first FVT was excluded in the figures to  
199 increase the visualisation. HF = high-fat, LF = low-fat, Amp = ampicillin, ns = not significant. \* =  $p < 0.05$ , \*\* =  $p < 0.006$ ,  
200 \*\*\* =  $p < 0.0005$ , \*\*\*\* =  $p < 0.0001$ .*

201

202 **FVT enhances the expression of genes involved in whole-body and energy**  
203 **homeostasis**

204 Gene expression panels were designed to target genes relevant for obesity and T2D in liver and  
205 ileum tissue to measure if the expression of these genes in the HF+FVT mice were significantly  
206 different to the HF mice, while being comparable to the LF mice. These conditions were  
207 represented by several genes involved in whole-body and energy homeostasis (Figure 3). Gene  
208 expression analysis suggested that the FVT had blunted the differences in gene expression  
209 caused by the HF diet resulting in an expression profile closer resembling that of the healthy LF  
210 mice. The expression levels of *Lepr*<sup>Liver</sup>, *Ffar2*<sup>Ileum</sup>, *Klb*<sup>Liver</sup>, *Ppargc1a*<sup>Liver</sup>, and *Igfbp2*<sup>Liver</sup> were  
211 significantly increased in the HF+FVT compared to the HF mice, whereas *Socs3*<sup>Liver</sup> and *Myc*<sup>Liver</sup>  
212 were significantly decreased (Figure 3). Generally, the gene expression levels (except *Socs3*<sup>Liver</sup>) in  
213 the HF+FVT mice fell between the levels observed in the LF and HF mice. Significant differences  
214 ( $p < 0.05$ ) were observed in the expression of several other genes (57 of 74 for liver tissue and 58  
215 of 74 for ileum tissue) between the experimental groups (see TableS3 for complete list).



216

217 *Figure 3: Gene expression levels at termination (18 weeks old) of a) *Lepr*<sup>Liver</sup> (leptin cytokine receptors), b) *Ffar2*<sup>Ileum</sup> (free*

218 fatty acid receptor), c) *Klb*<sup>Liver</sup> (Beta-klotho), d) *Ppargc1a*<sup>Liver</sup> (Peroxisome proliferator-activated receptor gamma

219 coactivator 1-alpha), e) *Igfbp2*<sup>Liver</sup> (insulin like growth factor binding protein), f) *Socs3*<sup>Liver</sup> (suppressor of cytokine

220 signalling), and g) *Myc*<sup>Liver</sup> (transcription factor). Linear models (one-way ANOVA) with either HF or LF as control groups

221 was performed to calculate group significance. The log2 fold change is a measure of the relative gene expression and is

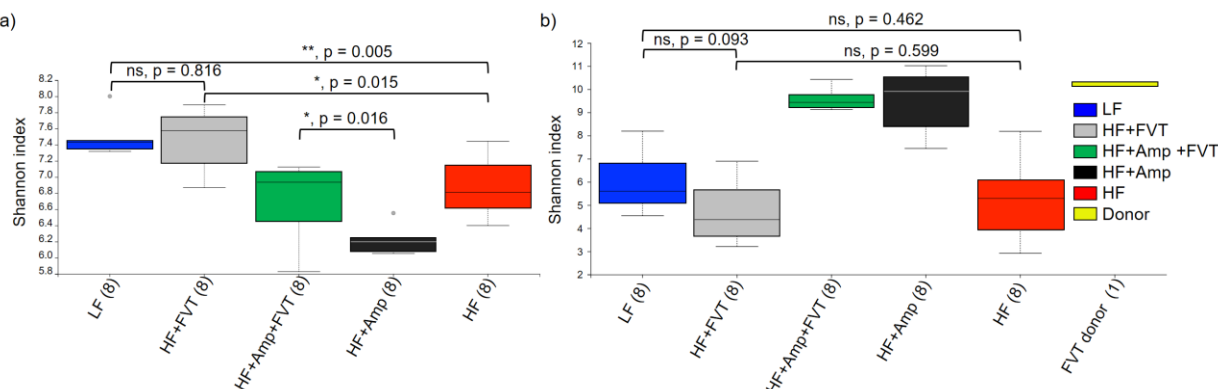
222 based on log2 transformed expression values normalised to the sample with the lowest value. HF = high-fat, LF = low-

223 fat, Amp = ampicillin, FVT = faecal virome transplantation.

224

## 225 FVT-mediated shift in the gut microbiota component

At termination the number of 16S rRNA gene copies/g of the cecum samples varied from 1.46 x 10<sup>10</sup> – 2.70 x 10<sup>10</sup> (FigureS3). The bacterial Shannon diversity index of the LF mice was significantly higher than the HF mice ( $p < 0.005$ ) but similar to the HF+FVT mice ( $p = 0.816$ ). The ampicillin-treated HF+Amp mice had the lowest Shannon diversity index of all groups at termination (i.e. 7 weeks after treatment with ampicillin) – and FVT increased the Shannon diversity index of ampicillin treated HF+Amp+FVT mice ( $p < 0.016$ ) (Figure 4a). The FVT had no significant ( $p > 0.09$ ) impact on the viral Shannon index, whereas the ampicillin treatment significantly ( $p < 0.0003$ ) increased the viral Shannon index (Figure 4b), possibly due to induction of prophages (FigureS6).

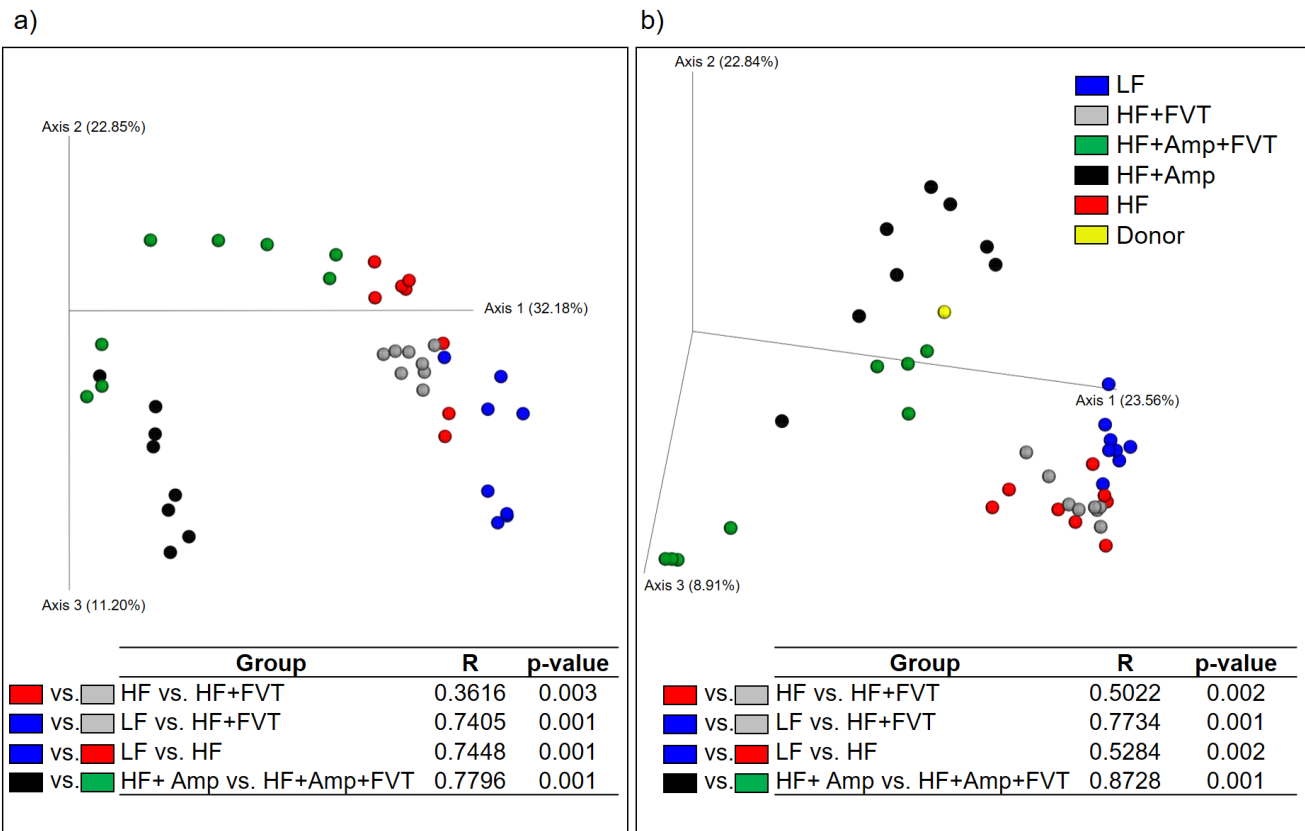


235

236 *Figure 4: Shannon index of the caecal a) bacterial and b) viral community at termination (18 weeks old). The*  
 237 *parentheses show the number of samples from each group included in the plot and grey dots indicate outliers. HF =*  
 238 *high-fat, LF = low-fat, Amp = ampicillin, FVT = faecal virome transplantation, ns = not significant. \* =  $p < 0.05$ , \*\* =  $p <$*   
 239 *0.0051.*

240 The FVT strongly influenced both the bacterial (Figure 5a,  $p < 0.003$ ) and viral (Figure 5b,  $p <$   
241  $0.001$ ) composition as determined by the Bray-Curtis dissimilarity-metric, as illustrated by a clear  
242 separation of the HF+FVT compared with the HF mice and HF+Amp+FVT with the HF+Amp mice.  
243 Further, all experimental groups were pairwise significantly separated ( $p < 0.003$ ) in both the viral  
244 and bacterial community (TableS4), including LF vs. HF+FVT ( $p < 0.001$ ). Overall, our findings  
245 suggest that FVT strongly influenced and partly reshape the GM composition both with and without  
246 ampicillin treatment.

247



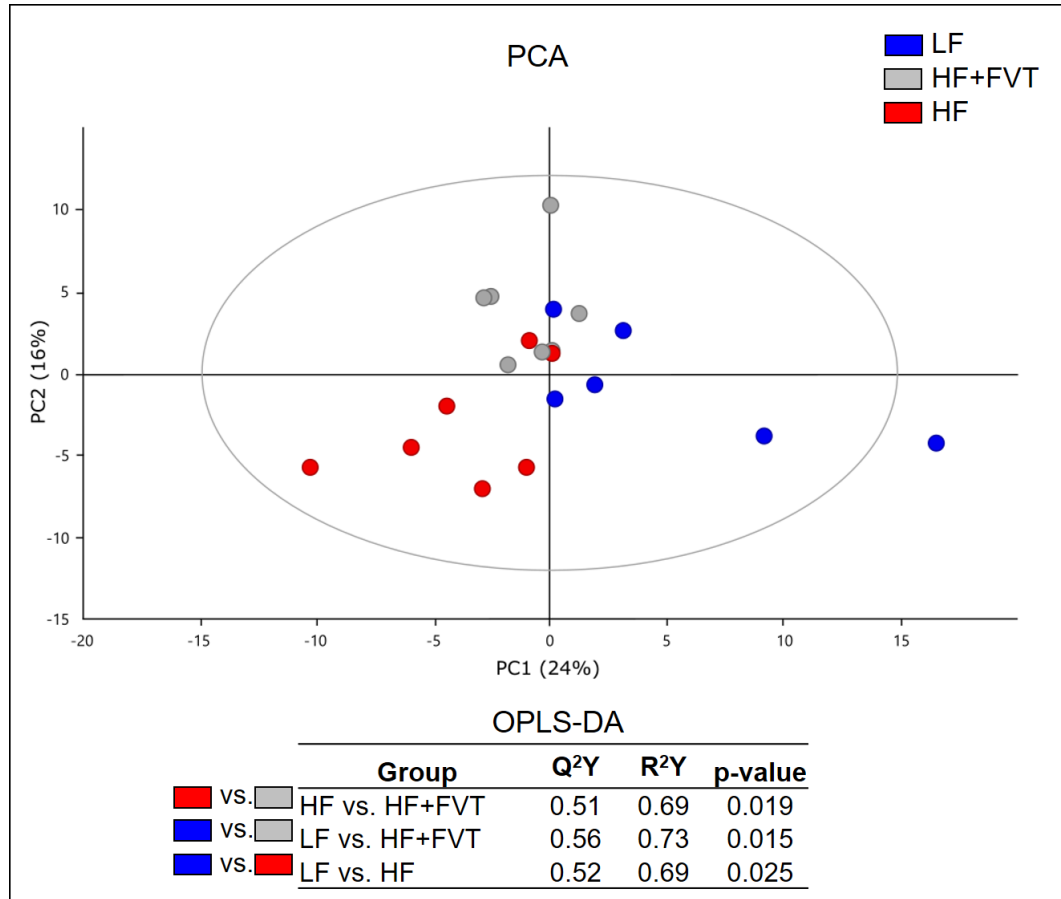
248

249 *Figure 5: Bray Curtis dissimilarity metric PCoA based plots of a) the caecal bacterial community and b) viral community*  
250 *at termination (18 weeks old). Tables include ANOSIM of the Bray Curtis dissimilarity to show the effect of the faecal*  
251 *virome transplantation (FVT) on the gut microbiota (GM) composition. HF = high-fat, LF = low-fat, Amp = ampicillin.*

252 **FVT-mediated shift in the blood plasma metabolome profile**

253 The influence of FVT on host metabolome was determined by untargeted UPLC-MS analysis of  
254 plasma samples. A PCA model was built on a refined dataset comparing LF, HF and HF+FVT  
255 profiles (Figure 6 and FigureS5 for all groups). Consistent with the other measures, the plasma  
256 profiles of HF+FVT mice were positioned between the HF and LF mice. Pairwise OPLS-DA models  
257 were constructed and all the models (LF vs. HF, LF vs. HF+FVT, HF vs. HF+FVT) were significant  
258 ( $p < 0.025$ ), supporting the separation of the three groups. Among the selected features with a VIP  
259 score  $> 2$ , only those correlating with relevant gene expression (based on rCCA), bacterial or viral  
260 abundance were further investigated for annotation. These features investigated consisted mainly  
261 of saturated and unsaturated lyso-phosphatidylcholine (LysoPC) and/or phosphatidylcholines  
262 (PCs), whereas the remaining features consisted of varieties of amino acids or unidentifiable  
263 metabolites (Table S5). Overall the HF mice had higher levels of LysoPC(18:2), LysoPC(22:2), and  
264 PC(16:0/22:6) than the LF mice which on the other hand had higher plasma levels of LysoPC(22:4)  
265 and PC(18:1/O-18:2). The HF+FVT mice had increased levels of circulating LysoPC(16:0),  
266 LysoPC(18:2), and PC(16:0/22:6) compared to the LF mice while the levels of LysoPC(22:4) and  
267 PC(18:1/O-18:2) were decreased. Further, the HF+FVT mice appeared with higher levels of

268 LysoPC(16:0), LysoPC(18:0), and PC(18:1/O-18:2) compared to the HF mice, whereas the LF  
269 mice showed higher levels of LysoPC(22:4) and PC(18:1/O-18:2) compared to the HF mice.



270

271 *Figure 6: PCA scores plot obtained from ESI+ UPLC-MS of plasma from LF, HF and HF+FVT (R<sup>2</sup>=0.40 and Q<sup>2</sup>=0.11) at*  
272 *termination (18 weeks old). Table includes supervised OPLS-DA models generated by pairwise comparisons. HF = high-*  
273 *fat, LF = low-fat, Amp = ampicillin.*

## 274 DISCUSSION

275 FVT has been successfully used to treat rCDI[14], an effect probably mediated by the ability of FVT  
276 to reshape the GM of the recipient. However, several parameters differentiate obesity and T2D  
277 from rCDI to which is characterised by a clonal infection highly susceptible to viral attack, a highly  
278 dysbiotic GM and the extensive use of antibiotics[14]. Here, we show that FVT from lean mice  
279 donors to obese recipients successfully counteracts some of the adverse effects of a HF diet with a  
280 decrease in body weight gain ( $p < 0.0034$ ) and a normalised blood glucose tolerance relative to  
281 mice fed a LF diet. Indeed, HF+FVT mice showed exactly the same response in an OGTT as the  
282 LF mice ( $p > 0.842$ , Figure 2), whereas similar effects were not observed in the HF+Amp+FVT  
283 mice. As expected[36], the diversity of the caecal bacterial community ( $\alpha$ -diversity) in the HF mice  
284 was significantly ( $p < 0.005$ ) lower compared to LF mice, but surprisingly the bacterial diversity of  
285 the HF+FVT was similar to the LF ( $p > 0.81$ ) and elevated in comparison ( $p < 0.015$ ) to the HF

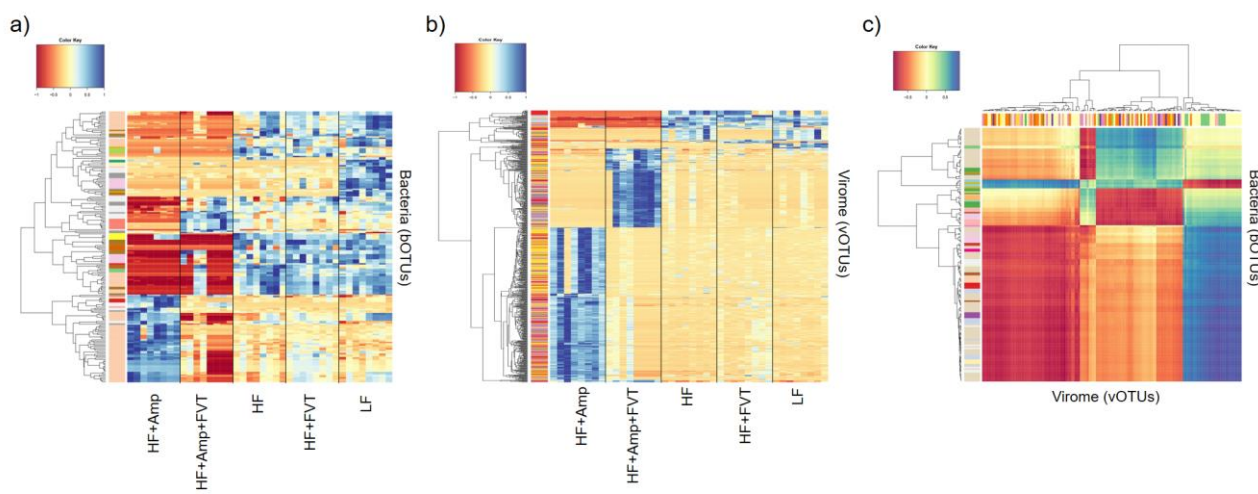
286 mice. No significant viral diversity differences were observed between LF vs. HF, LF vs. HF+FVT,  
287 and HF vs. HF+FVT. The significantly increased ( $p < 0.003$ ) diversity of the viral community in the  
288 ampicillin treated mice (Figure 4b) was likely due to induction of prophages[37], as indicated by an  
289 increased ( $p < 0.05$ ) presence of viral contigs containing integrase genes in the ampicillin treated  
290 groups (FigureS6). The composition of the viral community was dominated by order Caudovirales  
291 and family *Microviridae* viruses, which is in accordance with former studies investigating the enteric  
292 viral community in mammals[9,12]. The FVT strongly influenced both the bacterial and viral GM  
293 composition (Figure 5), with HF+FVT being significantly ( $p < 0.003$ ) different from both the HF as  
294 well as the LF mice. The highly diverse donor virome[17] as well as the distinct nutrition profiles  
295 (HF-diet vs. LF-diet) most likely explain the divergence in the GM composition profiles between the  
296 HF+FVT and the LF mice.

297 Gene expression analysis of obesity and T2D associated genes in liver and ileum showed that  
298 seven relevant genes (Figure 3) were differentially expressed ( $p < 0.05$ ) between HF+FVT and HF  
299 mice. The *Ffar2* gene is involved in energy homeostasis and can influence glucose homeostasis  
300 through GLP-1 regulation and leptin production[38,39], which might lower food intake and via GLP-  
301 1 decrease blood glucose levels by enhancing the production of insulin[38]. The *Ffar2* gene may  
302 also influence whole-body homeostasis through regulation of adipogenesis and lipid storage of  
303 adipocytes[40]. The expression of *Ffar2*<sup>ileum</sup> was comparable between LF and HF+FVT while in the  
304 HF mice expression was clearly reduced (Figure 3a). The *Lepr* genes are involved in the regulation  
305 of food intake, and *Lepr* deficient subjects rapidly increase body weight[41]. *Klb* contributes to the  
306 repression of cholesterol 7-alpha-hydroxylase and thereby regulate bile acid synthesis[42] with  
307 reduced expression in obese subjects[43]. *Ppargc1a* expression has been reported to be reduced  
308 and linked with islet insulin secretion in T2D patients[44], as well as playing a pivotal role in  
309 regulating energy homeostasis[45]. *Igfbp2* is involved in the insulin-like growth factor-axis  
310 influencing cell growth and proliferation[46] and high expression levels have been linked to the  
311 protection against T2D in human studies[47]. The gene expression of *Lepr*<sup>Liver</sup> (Figure3b), *Klb*<sup>Liver</sup>  
312 (Figure3c), *Ppargc1a*<sup>Liver</sup> (Figure3d), and *Igfbp2*<sup>Liver</sup> (Figure3e) were all significantly increased in the  
313 LF and HF+FVT mice compared to the HF mice. Knock-out of *Socs* genes have been reported to  
314 prevent insulin resistance in obesity as the result of a decrease in ceramide synthesis[48]. The  
315 *Socs3*<sup>Liver</sup> levels were significantly ( $p < 0.0001$ ) decreased in HF+FVT compared to both HF and LF  
316 mice (Figure 3f). However, the overall *Socs3*<sup>Liver</sup> levels in the LF mice was affected by high inter-  
317 group variation. The expression of *Myc* has been found to be increased in mice provided HF diet,  
318 and a decrease in bodyweight was obtained with haploin-sufficient mice (*c-Myc*<sup>+/−</sup>)[49]. The  
319 expression of *Myc*<sup>Liver</sup> was comparable between LF and HF+FVT while in the HF mice expression  
320 was clearly increased (Figure 3g). Overall, these findings indicate that FVT treatment affects the

321 expression of genes involved in stimulating appetite, blood glucose tolerance, and whole-body and  
322 energy homeostasis.

323 An extensive study of metabolic syndrome in humans, showed strong correlations between certain  
324 blood plasma metabolites and the GM component[50], and some of these correlations appear  
325 specific to the pre-diabetic state[50]. Furthermore, blood plasma metabolome seem to predict the  
326 GM diversity[51]. The blood plasma metabolome profile of the HF+FVT mice differed significantly  
327 ( $p < 0.025$ ) from both the LF and HF mice. SCFAs are expected to regulate the *Ffar2* gene[52] but  
328 our feature annotation did not detect any clear differences in circulating SCFAs between treatment  
329 groups. Further, Lysophosphatidylcholines are reduced in obesity and T2D[53], and we indeed observed a  
330 decrease in Lysophosphatidylcholines levels when comparing the HF with HF+FVT group and HF with the LF  
331 group, although the results were not clear. The beneficial effects associated to FVT were knocked  
332 down by the ampicillin treatment (except for weight gain), which was also reduced in the HF+Amp  
333 relative to HF, but the FVT consistently reshaped the GM composition profile in the HF+Amp+FVT  
334 mice as well.

335 Regularized Canonical Correlation Analysis (rCCA) suggested potential host-phage pair relations  
336 by strong ( $r > 0.75$ ) positive and negative correlations between certain bacterial (order  
337 Bacteroidales, Clostridiales) and viral (order Caudovirales, family *Microviridae* and uncharacterised  
338 viruses) taxa. Likewise, random forest selected variables showed bacterial and viral co-abundance  
339 profiles that differentiated the five experimental groups (Figure 7) supporting the effect of the FVT  
340 on the GM component.



341

342 *Figure 7: Heatmaps illustrating the bacterial a) and viral b) profile of all five experimental groups, as well as strong*  
343 *correlations between certain clusters of bacteria and viruses c). Detailed information and high-resolution images can be*  
344 *found as supplemental materials in Figure S7 and S8.*

345 Zuo *et al.*[54] investigated how the phage community could be related to the effect of FMT against  
346 rCDI and found that a few patients did not respond on the treatment. The common denominator of  
347 the patients that did respond on the FMT treatment was that the Caudovirales richness in the  
348 donor faeces was higher than the Caudovirales richness in the recipient, whereas most of the non-  
349 responder recipients had a higher Caudovirales richness than the donor. Based on these findings,  
350 Zuo *et al.* hypothesised that a higher Caudovirales richness in the donor compared to the recipient  
351 is important for a successful FMT treatment[54]. The Caudovirales richness of the FVT donor  
352 virome in our study (faecal virome from mice purchased at three different vendors[17]) was higher  
353 than any of the recipient groups at termination (FigureS9). Whereas the Caudovirales richness of  
354 the viromes from the individual mouse vendors were notably less compared to the FVT virome and  
355 both recipient groups. Although further studies are needed, these findings are consistent with those  
356 of Zuo *et al.* and suggests that a virome from a single vendor/donor might not have the same effect  
357 as when multiple viromes are combined for FVT.

358 We expect that phages transferred with the FVT in the HF+FVT mice have reshaped the GM  
359 component and thereby shifted the phenotype of the obese HF mice to be in closer resemblance of  
360 the lean LF mice. This hypothesis seems plausible since several recent studies have reported a  
361 correlation between phage diversity and intestinal microbiome diversity[12], a FVT-mediated  
362 restoration of the GM of antibiotic treated mice[15], and a phage-mediated shift in the gut  
363 metabolome profile[13].

364 In conclusion, we here demonstrate the use of FVT targeting obesity and T2D in an animal model.  
365 Although the study is a proof-of-concept, our findings highlight the potential of using phage-  
366 mediated therapy against obesity and T2D[6] that represents a world-wide health threat[1].

### 367 **Acknowledgement**

368 Thanks to Julie Mou Larsen for assisting with sampling of mouse tissue and associated method  
369 description. In addition, we thank Helene Farlov, Mette Nelander at Section of Experimental Animal  
370 Models and Liv de Vries at Section for Microbiology and Fermentation (University of Copenhagen,  
371 Denmark) for taking care of the animals. We thank Helle Keinicke and Marina Kjærgaard  
372 Gerstenberg for selecting the genes and providing the primers for the liver gene expression panel.

### 373 **Contributors**

374 T.S.R., C.M.M., A.K.H., D.S.N, and F.K.V. conceived the research idea and designed the study;  
375 C.M.M. and T.S.R. performed the animal experiments; T.S.R., C.M.M., and S.Z. processed the  
376 samples in the laboratory; T.S.R., C.M.M., L.H.H., W.K., D.S.N, J.S., S.Z., J.C.M., and F.K.V  
377 performed data analysis; T.S.R. and D.S.N was responsible for the first and final draft of the

378 manuscript, as well as all requested revisions. All authors critically revised and approved the final  
379 version of the manuscript.

380 **Competing interests**

381 All authors declare no conflicts of interest.

382 **Funding**

383 Funding was provided by the Danish Council for Independent Research with grant ID: DFF-6111-  
384 00316 (PhageGut) and the Danish Innovation Fund project - 7076-00129B, MICROHEALTH.

385 **References**

- 386 1 Leitner DR, Frühbeck G, Yumuk V, *et al.* Obesity and type 2 diabetes: Two diseases with a  
387 need for combined treatment strategies - EASO can lead the way. *Obes Facts*  
388 2017;**10**:483–92. doi:10.1159/000480525
- 389 2 Maruvada P, Leone V, Kaplan LM, *et al.* The Human Microbiome and Obesity: Moving  
390 beyond Associations. *Cell Host Microbe* 2017;**22**:589–99. doi:10.1016/j.chom.2017.10.005
- 391 3 Cho I, Yamanishi S, Cox L, *et al.* Antibiotics in early life alter the murine colonic microbiome  
392 and adiposity. *Nature* 2012;**488**:621–6. doi:10.1038/nature11400
- 393 4 Ridaura VK, Faith JJ, Rey FE, *et al.* Gut microbiota from twins discordant for obesity  
394 modulate metabolism in mice. *Science (80- )* 2013;**341**:1241214.  
395 doi:10.1126/science.1241214
- 396 5 Kelly CR, Kahn S, Kashyap P, *et al.* Update on Fecal Microbiota Transplantation 2015:  
397 Indications, Methodologies, Mechanisms, and Outlook. *Gastroenterology* 2015;**149**:223–37.  
398 doi:10.1053/j.gastro.2015.05.008
- 399 6 Gupta S, Allen-vercoe E, Petrof EO. Fecal microbiota transplantation : in perspective.  
400 *Therap Adv Gastroenterol* 2016;**9**:229–39. doi:10.1177/1756283X15607414
- 401 7 Wang JYJWJYJW, Kuo CH, Kuo FC, *et al.* Fecal microbiota transplantation: Review and  
402 update. *J Formos Med Assoc* 2019;**118**:S23–31. doi:10.1016/j.jfma.2018.08.011
- 403 8 FDA. FDA - Important Safety Alert Regarding Use of Fecal Microbiota for Transplantation  
404 and Risk of Serious Adverse Reactions Due to Transmission of Multi-Drug Resistant  
405 Organisms. 2019. <https://www.fda.gov/vaccines-blood-biologics/safety-availability-biologics/important-safety-alert-regarding-use-fecal-microbiota-transplantation-and-risk-serious-adverse> (accessed 4 Jul 2019).
- 408 9 Reyes A, Haynes M, Hanson N, *et al.* Viruses in the faecal microbiota of monozygotic twins  
409 and their mothers. *Nature* 2011;**466**:334–8. doi:10.1038/nature09199
- 410 10 Ross A, Ward S, Hyman P. More Is Better : Selecting for Broad Host Range  
411 Bacteriophages. 2016;**7**:1–6. doi:10.3389/fmicb.2016.01352
- 412 11 Howe A, Ringus DL, Williams RJ, *et al.* Divergent responses of viral and bacterial  
413 communities in the gut microbiome to dietary disturbances in mice. *ISME J* 2016;**10**:1217–  
414 27. doi:10.1038/ismej.2015.183
- 415 12 Moreno-Gallego JL, Chou SP, Di Rienzi SC, *et al.* Virome Diversity Correlates with Intestinal

- 416 12 Microbiome Diversity in Adult Monozygotic Twins. *Cell Host Microbe* 2019;25:261-272.e5.  
417 doi:10.1016/j.chom.2019.01.019
- 418 13 Hsu BB, Gibson TE, Yeliseyev V, et al. Dynamic Modulation of the Gut Microbiota and  
419 Metabolome by Bacteriophages in a Mouse Model. *Cell Host Microbe* 2019;25:803-814.e5.  
420 doi:10.1016/j.chom.2019.05.001
- 421 14 Ott SJ, Waetzig GH, Rehman A, et al. Efficacy of Sterile Fecal Filtrate Transfer for Treating  
422 Patients With Clostridium difficile Infection. *Gastroenterology* 2017;152:799–811.  
423 doi:10.1053/j.gastro.2016.11.010
- 424 15 Draper LA, Ryan FJ, Dalmasso M, et al. Autochthonous faecal virome transplantation (FVT)  
425 reshapes the murine microbiome after antibiotic perturbation. *bioRxiv* 2019;:591099.  
426 doi:10.1101/591099
- 427 16 Fraulob JC, Ogg-Diamantino R, Fernandes-Santos C, et al. A Mouse Model of Metabolic  
428 Syndrome: Insulin Resistance, Fatty Liver and Non-Alcoholic Fatty Pancreas Disease  
429 (NAFPD) in C57BL/6 Mice Fed a High Fat Diet. *J Clin Biochem Nutr* 2010;46:212–23.  
430 doi:10.3164/jcbn.09-83
- 431 17 Rasmussen TS, de Vries L, Kot W, et al. Mouse Vendor Influence on the Bacterial and Viral  
432 Gut Composition Exceeds the Effect of Diet. *Viruses* 2019;11:435. doi:10.3390/v11050435
- 433 18 Rune I, Rolin B, Lykkesfeldt J, et al. Long-term Western diet fed apolipoprotein E-deficient  
434 rats exhibit only modest early atherosclerotic characteristics. *Sci Rep* 2018;8:1–12.  
435 doi:10.1038/s41598-018-23835-z
- 436 19 Krych Ł, Kot W, Bendtsen KMB, et al. Have you tried spermine ? A rapid and cost-effective  
437 method to eliminate dextran sodium sulfate inhibition of PCR and RT-PCR. *J Microbiol  
438 Methods* J 2018;144:1–7. doi:10.1016/j.mimet.2017.10.015
- 439 20 Ellekilde M, Krych Ł, Hansen CHFHF, et al. Characterization of the gut microbiota in leptin  
440 deficient obese mice - Correlation to inflammatory and diabetic parameters. *Res Vet Sci*  
441 2014;96:241–50. doi:10.1016/j.rvsc.2014.01.007
- 442 21 Bolger AM, Lohse M, Usadel B. Trimmomatic: A flexible trimmer for Illumina sequence data.  
443 *Bioinformatics* 2014;30:2114–20. doi:10.1093/bioinformatics/btu170
- 444 22 Edgar RC. UPARSE: highly accurate OTU sequences from microbial amplicon reads. *Nat  
445 Methods* 2013;10:996–8. doi:10.1038/nmeth.2604
- 446 23 Bankevich A, Nurk S, Antipov D, et al. SPAdes: A new genome assembly algorithm and its  
447 applications to single-cell sequencing. *J Comput Biol* 2012;19:455–77.  
448 doi:10.1089/cmb.2012.0021
- 449 24 Nurk S, Meleshko D, Korobeynikov A, et al. metaSPAdes: a new versatile metagenomic  
450 assembler. *Genome Res* 2017;27:824–34. doi:10.1101/gr.213959.116
- 451 25 Wood DE, Salzberg SL. Kraken: ultrafast metagenomic sequence classification using exact  
452 alignments. *Genome Biol* 2014;15:R46. doi:10.1186/gb-2014-15-3-r46
- 453 26 Ren J, Ahlgren NA, Lu YY, et al. VirFinder: a novel k-mer based tool for identifying viral  
454 sequences from assembled metagenomic data. *Microbiome* 2017;5:69. doi:10.1186/s40168-  
455 017-0283-5
- 456 27 Arndt D, Grant JR, Marcu A, et al. PHASTER: a better, faster version of the PHAST phage  
457 search tool. *Nucleic Acids Res* 2016;44:1–6. doi:10.1093/nar/gkw387

- 458 28 Bendtsen KM, Hansen CHF, Krych Ł, et al. Immunological effects of reduced mucosal  
459 integrity in the early life of BALB/c mice. *PLoS One* 2017;12:1–20.  
460 doi:10.1371/journal.pone.0176662
- 461 29 Zachariassen LF, Krych L, Rasmussen SH, et al. Cesarean Section Induces Microbiota-  
462 Regulated Immune Disturbances in C57BL/6 Mice. *J Immunol* 2019;202:142–50.  
463 doi:10.4049/jimmunol.1800666
- 464 30 Mentzel CMJ, Cardoso TF, Pipper CB, et al. Deregulation of obesity-relevant genes is  
465 associated with progression in BMI and the amount of adipose tissue in pigs. *Mol Genet  
466 Genomics* 2018;293:129–36. doi:10.1007/s00438-017-1369-2
- 467 31 Sarafian MH, Gaudin M, Lewis MR, et al. Objective Set of Criteria for Optimization of  
468 Sample Preparation Procedures for Ultra-High Throughput Untargeted Blood Plasma Lipid  
469 Profiling by Ultra Performance Liquid Chromatography–Mass Spectrometry. *Anal Chem*  
470 2014;86:5766–74. doi:10.1021/ac500317c
- 471 32 Roux S, Emerson JB, Eloe-Fadrosch EA, et al. Benchmarking viromics: an *in silico* evaluation  
472 of metagenome-enabled estimates of viral community composition and diversity. *PeerJ*  
473 2017;5:e3817. doi:10.7717/peerj.3817
- 474 33 Rohart F, Gautier B, Singh A, et al. mixOmics: An R package for ‘omics feature selection  
475 and multiple data integration. *PLOS Comput Biol* 2017;13:e1005752.  
476 doi:10.1371/journal.pcbi.1005752
- 477 34 Breiman L. Random forests. *Mach Learn* 2001;45:5–32. doi:10.1023/A:1010933404324
- 478 35 Zhao S, Guo Y, Sheng Q, et al. Heatmap3: An improved heatmap package with more  
479 powerful and convenient features. *BMC Bioinformatics* 2014;15:P16. doi:10.1186/1471-  
480 2105-15-S10-P16
- 481 36 Sun L, Ma L, Ma Y, et al. Insights into the role of gut microbiota in obesity: pathogenesis,  
482 mechanisms, and therapeutic perspectives. *Protein Cell* 2018;9:397–403.  
483 doi:10.1007/s13238-018-0546-3
- 484 37 Allen HK, Loof T, Bayles DO, et al. Antibiotics in feed induce prophages in swine fecal  
485 microbiomes. *MBio* 2011;2:1–9. doi:10.1128/mBio.00260-11
- 486 38 Hudson BD, Due-Hansen ME, Christiansen E, et al. Defining the molecular basis for the first  
487 potent and selective orthosteric agonists of the FFA2 free fatty acid receptor. *J Biol Chem*  
488 2013;288:17296–312. doi:10.1074/jbc.M113.455337
- 489 39 Ichimura A, Hasegawa S, Kasubuchi M, et al. Free fatty acid receptors as therapeutic  
490 targets for the treatment of diabetes. *Front Pharmacol* 2014;5:1–6.  
491 doi:10.3389/fphar.2014.00236
- 492 40 Murdock PR, Pike NB, Eilert MM, et al. The Orphan G Protein-coupled Receptors GPR41  
493 and GPR43 Are Activated by Propionate and Other Short Chain Carboxylic Acids. *J Biol  
494 Chem* 2003;278:11312–9. doi:10.1074/jbc.m211609200
- 495 41 Dubern B, Clement K. Leptin and leptin receptor-related monogenic obesity. *Biochimie*  
496 2012;94:2111–5. doi:10.1016/j.biochi.2012.05.010
- 497 42 Ito S, Fujimori T, Furuya A, et al. Impaired negative feedback suppression of bile acid  
498 synthesis in mice lacking βKlotho. *J Clin Invest* 2005;115:2202–8. doi:10.1172/JCI23076
- 499 43 Kruse R, Vienberg SG, Vind BF, et al. Effects of insulin and exercise training on FGF21, its  
500 receptors and target genes in obesity and type 2 diabetes. *Diabetologia* 2017;60:2042–51.

- 501 doi:10.1007/s00125-017-4373-5

502 44 Ling C, Del Guerra S, Lupi R, *et al.* Epigenetic regulation of PPARGC1A in human type 2  
503 diabetic islets and effect on insulin secretion. *Diabetologia* 2008;51:615–22.  
504 doi:10.1007/s00125-007-0916-5

505 45 Charos AE, Reed BD, Raha D, *et al.* A highly integrated and complex PPARGC1A  
506 transcription factor binding network in HepG2 cells. *Genome Res* 2012;22:1668–79.  
507 doi:10.1101/gr.127761.111

508 46 Rajpathak SN, Gunter MJ, Wylie-Rosett J, *et al.* The role of insulin-like growth factor-I and  
509 its binding proteins in glucose homeostasis and type 2 diabetes. *Diabetes Metab Res Rev*  
510 2009;25:3–12. doi:10.1002/dmrr.919

511 47 Wittenbecher C, Ouni M, Kuxhaus O, *et al.* Insulin-like growth factor binding protein 2  
512 (IGFBP-2) and the risk of developing type 2 diabetes. *Diabetes* 2019;68:188–97.  
513 doi:10.2337/db18-0620

514 48 Yang G, Badeanlou L, Bielawski J, *et al.* Central role of ceramide biosynthesis in body  
515 weight regulation, energy metabolism, and the metabolic syndrome. *Am J Physiol Metab*  
516 2009;297:E211–24. doi:10.1152/ajpendo.91014.2008

517 49 Liu S, Kim TH, Franklin DA, *et al.* Protection against High-Fat-Diet-Induced Obesity in  
518 MDM2C305F Mice Due to Reduced p53 Activity and Enhanced Energy Expenditure. *Cell*  
519 *Rep* 2017;18:1005–18. doi:10.1016/j.celrep.2016.12.086

520 50 Org E, Blum Y, Kasela S, *et al.* Relationships between gut microbiota, plasma metabolites,  
521 and metabolic syndrome traits in the METSIM cohort. *Genome Biol* 2017;18:1–14.  
522 doi:10.1186/s13059-017-1194-2

523 51 Wilmanski T, Rappaport N, Earls JC, *et al.* Blood metabolome predicts gut microbiome  $\alpha$ -  
524 diversity in humans. *Nat Biotechnol* 2019;37. doi:10.1038/s41587-019-0233-9

525 52 Le Poul E, Loison C, Struyf S, *et al.* Functional characterization of human receptors for short  
526 chain fatty acids and their role in polymorphonuclear cell activation. *J Biol Chem*  
527 2003;278:25481–9. doi:10.1074/jbc.M301403200

528 53 Barber MN, Risis S, Yang C, *et al.* Plasma lysophosphatidylcholine levels are reduced in  
529 obesity and type 2 diabetes. *PLoS One* 2012;7:1–12. doi:10.1371/journal.pone.0041456

530 54 Zuo T, Wong SH, Lam K, *et al.* Bacteriophage transfer during faecal microbiota  
531 transplantation in Clostridium difficile infection is associated with treatment outcome. *Gut*  
532 2018;67:634–43. doi:10.1136/gutjnl-2017-313952

533